*New Explorations in Electrical Engineering (NECE)*
*Department of Electrical Engineering,*
*Faculty of Engineering*
*Universiti Malaya, MALAYSIA*

*Vol. 2, No. 1 (2026)*
*pp. 2–11*

# Machine Learning-Based Structural Damage Identification Utilising Frequency Response Function Peak Amplitude Ratios

Bing Zhen Cheah[a], Zhi Chao Ong[a,b,*] , Shin Yee Khoo[a,b], Pei Yi Siow[a,b], Zainah Ibrahim[c] and Chee Ghuan Tan[c]

[a] *Department of Mechanical Engineering, Faculty of Engineering, Universiti Malaya, 50603 Kuala Lumpur, Malaysia*

[b] *Centre for Research in Industry 4.0 (CRI4.0), Faculty of Engineering, Universiti Malaya, 50603 Kuala Lumpur, Malaysia*

[c] *Department of Civil Engineering, Faculty of Engineering, Universiti Malaya, 50603 Kuala Lumpur, Malaysia*

**Abstract**. With the rapid advancement of technologies such as machine learning (ML) and edge computing, ML-integrated structural damage identification has gained significant traction. Modal-based methods are frequently preferred for these applications due to the inherent robustness of modal features. Frequency Response Functions (FRFs) obtained via experimental modal analysis are rich in damage-sensitive information; however, the resulting datasets often suffer from high dimensionality. This paper investigates the feasibility of employing dimensionally reduced features extracted from FRFs to train ML models, specifically to minimise computational overhead during the training phase. Experimental validation was conducted using a laboratory-scale plate test rig. The study evaluates the predictive accuracy, model size and training duration for three distinct feature sets: raw FRFs, FRF peak amplitudes, and FRF peak amplitude ratios. While all three feature sets maintained predictive accuracies above 99.5%, the FRF peak amplitude ratio set yielded the most compact model and the fastest training time. Therefore, utilizing the FRF peak amplitude ratio as a primary training feature provides an effective method to reduce computational overhead while preserving high accuracy in structural damage identification.

Keywords. Structural Damage Identification, Machine Learning, Modal Analysis, Frequency Response Function, Structural Health Monitoring

## 1. Introduction

The paradigm of structural maintenance has evolved significantly over recent decades, transitioning from traditional reactive and preventive strategies to the sophisticated domain of Predictive Maintenance (PdM). While preventive maintenance relies on scheduled intervals regardless of the actual state of the asset, PdM leverages real-time monitoring to anticipate failures before they occur. This shift minimizes unnecessary downtime and optimizes the lifecycle of critical infrastructure.

In the modern era, the efficacy of predictive maintenance is increasingly driven by Machine Learning (ML) (Bitam et al., 2025). The integration of ML algorithms enables the processing of vast datasets to identify complex patterns and anomalies that manual inspection might overlook. This synergy further enables automated structural health monitoring (SHM), offering advantages such as increased diagnostic

* Corresponding author. Email: alexongzc@um.edu.my

speed, the ability to handle non-linear data relationships, and enhanced scalability across diverse engineering structures.

To develop highly accurate ML models, the selection of suitable training features is paramount. Vibration-based features have consistently proven to be robust indicators of structural integrity (Mardanshahi et al., 2025); they remain relatively consistent and demonstrate resilience against slight variations in environmental conditions compared to raw time-domain signals.

Historically, Frequency Response Functions (FRF) have been widely adopted as primary training features (Ruiz et al., 2024). However, raw FRF data often presents a challenge due to its high dimensionality, which can lead to the 'curse of dimensionality' during model training. To mitigate this, Principal Component Analysis (PCA) is frequently employed to reduce dimensions, yielding PCA-FRF (Li et al., 2011).

Building upon dimension-reduction techniques, Chen et al. retrieved the Waveform Chain Code (WCC) feature from PCA-FRF. Research indicates that the WCC feature is highly sensitive to damage severity. However, assessing the location of damage requires additional indicators, as WCC alone lacks sufficient sensitivity toward spatial localization. Consequently, Mode Shape Difference (MSD) method has been utilised, which has shown efficacy in determining both location and severity (Siow et al., 2023). A drawback of MSD, however, is the requirement for curve-fitting the FRF to extract mode shapes. The curve-fitting process is essentially an estimation and might introduce potential errors, unlike values derived directly from the FRF.

Further refining feature selection, WCC has been paired with FRF peak amplitudes (PA) for the damage identification of plate-like structures, achieving high accuracy (Cheah et al., 2025). This underscores a critical objective in SHM: if highly representative features are selected, the total number of features can be reduced. Reducing the feature set not only accelerates the ML training process but also significantly lowers the memory requirements for data storage. It is quintessential, however, that these leaner models maintain high accuracy in damage identification to remain viable for real world applications.

In this paper, the application of a novel FRF Peak Amplitude Ratio (PAR) as machine learning training feature is investigated. The study evaluates this novel feature in terms of ML training time, model accuracy, and the storage space required for data and model management. To validate its performance, the proposed method was benchmarked against standard ML models trained using raw FRF magnitude and individual FRF PA.

## 2. Methods

### *2.1. Experimental setup and data acquisition*

A lab-scale acrylic plate structure with supports at 4 edges was experimented with as shown in Fig. 1. The FRF data was acquired by impact hammer test, using an impact hammer, 5 accelerometers, NI-9234 dynamic signal acquisition module, and a PC.

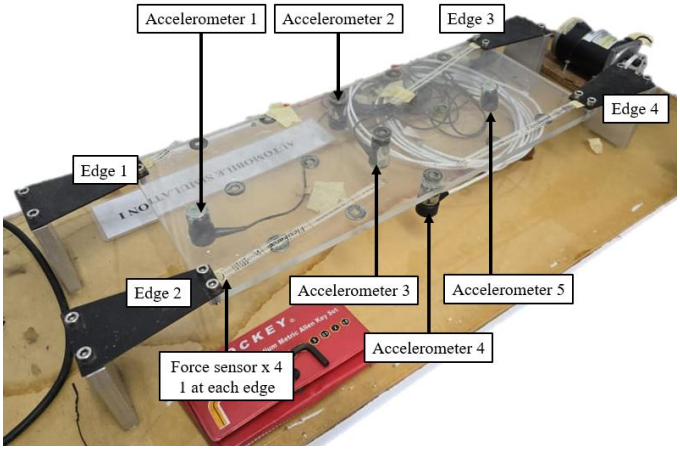


**Figure 1.** Lab-scale plate structure test rig.

FRFs were collected from impact hammer test under various damage condition. The damage was created by loosening of screws at the 4 edges. The damage severity was grouped into undamaged (UD), low severity damage (LD), medium severity damage (MD) and high severity damage (HD). The damage combination is as listed in Table 1.

**Table 1.** Damage classes.

| Class Abbreviation | Damage Severity | Damage Location | Force Sensor Reading (N) / Description | Number of Samples |
|---|---|---|---|---|
| UD | UD | N/A | 150 N | 10 |
| LD-1 | LD | Edge 1 | 113 N, 78 N, 38 N | 30 |
| LD-2 | LD | Edge 2 | 113 N, 78 N, 38 N | 30 |
| LD-3 | LD | Edge 3 | 113 N, 78 N, 38 N | 30 |
| LD-4 | LD | Edge 4 | 113 N, 78 N, 38 N | 30 |
| MD-1 | MD | Edge 1 | 0 N / both screws loosened and not removed; 1 screw loosened, and the other is removed | 20 |
| MD-2 | MD | Edge 2 | 0 N / both screws loosened and not removed; 1 screw loosened, and the other is removed | 20 |
| MD-3 | MD | Edge 3 | 0 N / both screws loosened and not removed; 1 screw loosened, and the other is removed | 20 |
| MD-4 | MD | Edge 4 | 0 N / both screws loosened and not removed; 1 screw loosened, and the other is removed | 20 |
| HD-1 | HD | Edge 1 | 0 N / both screws removed | 10 |
| HD-2 | HD | Edge 2 | 0 N / both screws removed | 10 |
| HD-3 | HD | Edge 3 | 0 N / both screws removed | 10 |
| HD-4 | HD | Edge 4 | 0 N / both screws removed | 10 |

## *2.2. Feature extraction and engineering*

With the collected input force $x(t)$ and output acceleration $y(t)$, the FRF was obtained from Eq. (1), where $H(f)$ is the FRF; $G_{xy}(f)$ is the cross-spectrum between input $x(t)$ and output y(t); $G_{xx}(f)$ is the auto-spectrum of input $x(t)$.

$$H(f) = \frac{G_{xy}(f)}{G_{xx}(f)} \quad (1)$$

Using PCA, the 5 FRFs which correspond to each measurement point, were reduced to 1 PCA-FRF by taking the principal component 1 (PC1). The PCA-FRF's waveform chain code (WCC) feature was computed by using UD as reference.

From the FRF, the peak amplitude (PA) of the first peak was retrieved, i.e. $A_1$, $A_2$, $A_3$, $A_4$ and $A_5$, where the subscript indicates the damaged edge location. The peak amplitude ratios, $PAR_{1,5}$ and $PAR_{2,4}$ were computed using Eqs (2) and (3).

$$PAR_{1,5} = \frac{A_1}{A_5} \quad (2)$$

$$PAR_{2,4} = \frac{A_2}{A_4} \quad (3)$$

### *2.3. Machine learning framework*

3 separate ML models were built to evaluate the performance of different set of features. As depicted in Table 2, three distinct feature sets were configured for evaluation: Feature Set 1 (FS1) consisted solely of raw FRF data; Feature Set 2 (FS2) incorporated WCC and FRF PA; and the proposed Feature Set 3 (FS3) utilised WCC combined with the novel FRF PAR. The features selected were based on frequency range 10 Hz to 25 Hz corresponding to the first mode.

**Table 2.** Feature sets for ML model.

| Feature Set | Features |
|---|---|
| FS1 | FRF |
| FS2 | WCC, FRF PA |
| FS3 | WCC, FRF PAR |

The ML model for damage identification was built using a feed forward neural network with backpropagation architecture. The network consisted of 4 layers (1 input layer, 2 hidden layers, 1 output layer). The hidden layers consisted of 256 neurons. ReLU was used as the hidden layer's activation function, while the output layer used softmax activation function. To optimize the network for multi-class classification, the model was compiled using the Adam (Adaptive Moment Estimation) optimisation algorithm. The objective function utilised was Categorical Crossentropy, which measures the performance of the classification model whose output is a probability value between 0 and 1.

To ensure robust performance evaluation, a repeated stratified k-fold cross-validation strategy was implemented. This approach utilised 10 repetitions of a 5-fold split, generating 50 distinct training and validation iterations.

### *2.4. Performance evaluation metrics*

Three distinct machine learning pipelines were developed to evaluate the feature sets detailed in Table 2. In each pipeline, the selected features were derived from the 10 Hz to 25 Hz frequency band, corresponding to the first mode. Performance metrics, including the mean model size, mean training duration and aggregated accuracy over the 50 iterations, were recorded for each pipeline.

## 3. Results and discussion

Fig. 2, Fig. 3 and Fig. 4 shows the acquired FRF under various damage conditions. The shift in FRF is greater with higher severity of damage, where the shift is most notable for HD cases, while there is minimal shift for LD cases. Hence, this suggests that FRF is sensitive to structural damage, especially high severity damage.

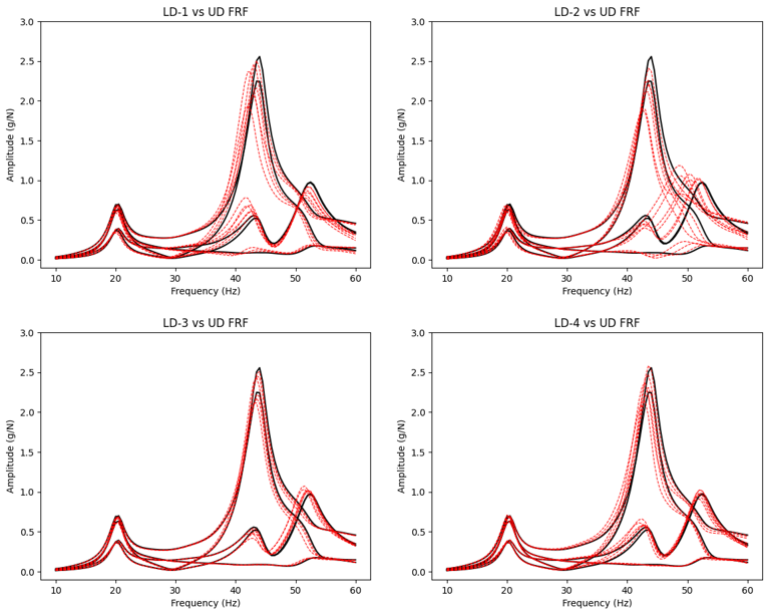


**Figure 2.** LD FRF (red dashed line) plotted against UD FRF (black solid line).

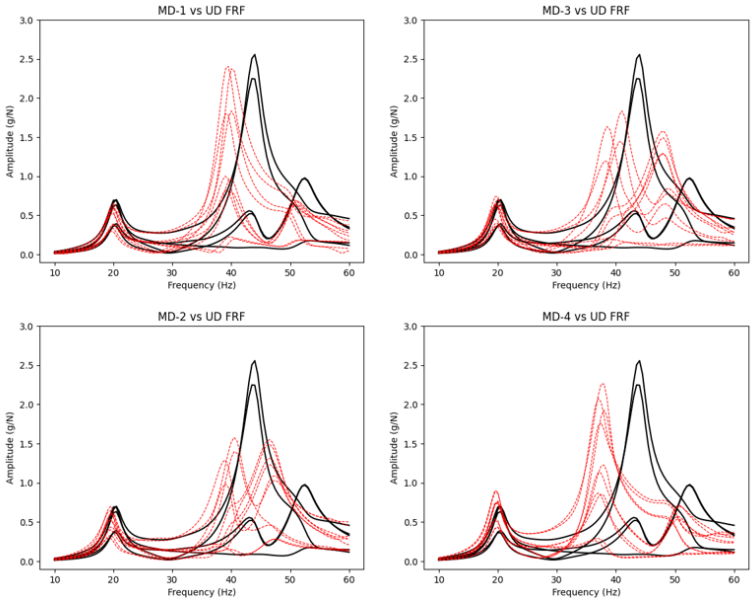


**Figure 3.** MD FRF (red dashed line) plotted against UD FRF (black solid line).

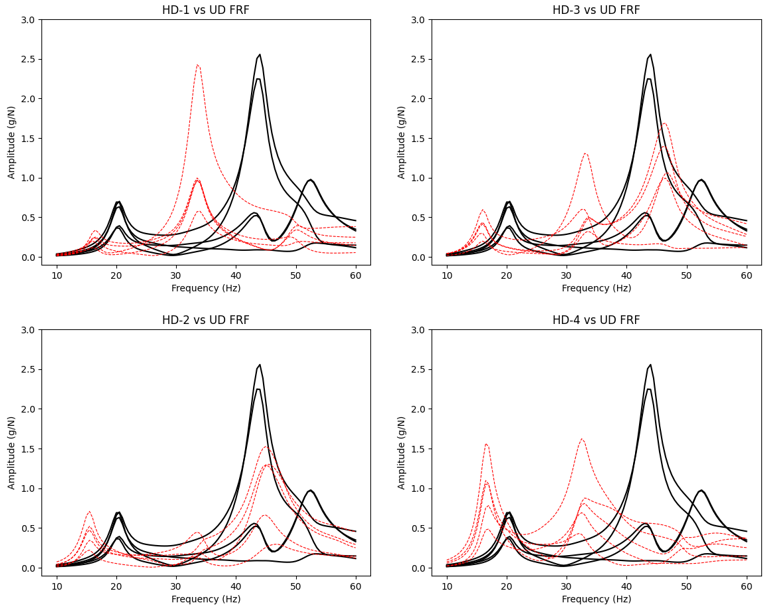


**Figure 4.** HD FRF (red dashed line) plotted against UD FRF (black solid line).

Fig. 5 shows the extracted FRF PARs. It is observed that values of $PAR_{1,5}$ is higher when damage happens at Edge 1 and Edge 2 compared to Edge 3 and Edge 4. On the other hand, values of $PAR_{2,4}$ is higher when damage happens at Edge 1 and Edge 3 compared to Edge 2 and Edge 4.

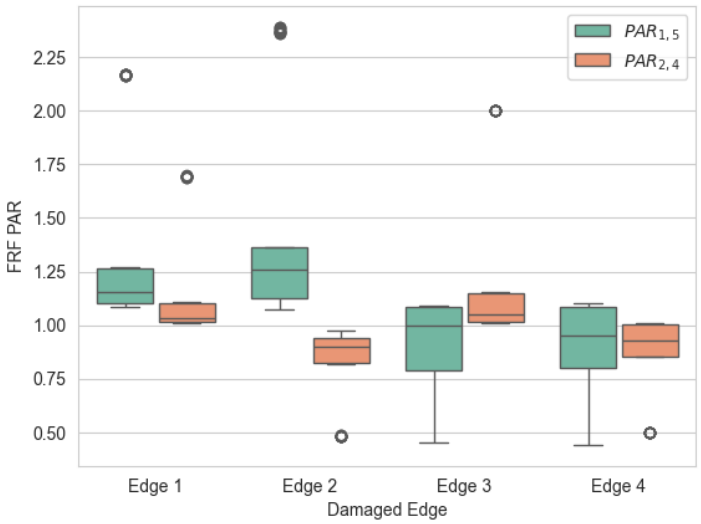


**Figure 5.** Boxplot of FRF PAR with varying damage location.

Fig. 6 shows WCC feature extracted from PCA FRF for frequency range 10 Hz – 25 Hz. It is evident that the WCC feature is sensitive to damage severity, hence it complements FRF PAR, which is sensitive

to damage location. Thus, both features if used together would offer good sensitivity towards both damage location and damage severity.

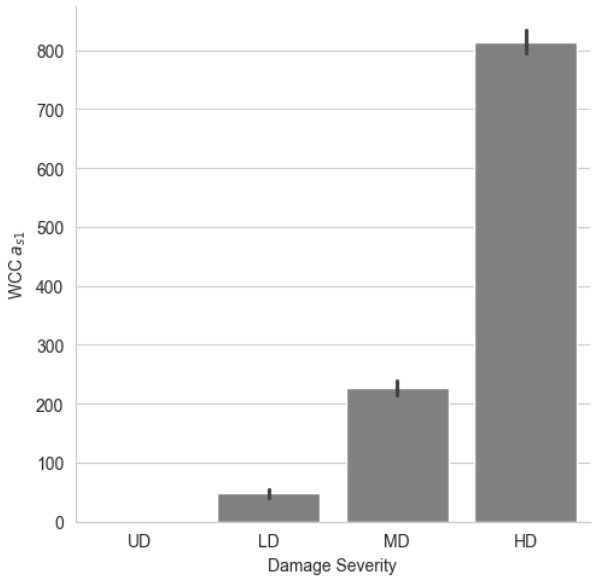


**Figure 6.** Boxplot of FRF PAR with varying damage location.

The experimental results, summarised in Table 3, demonstrate that all three feature sets achieved a highly robust prediction accuracy above 99.5% in identifying structural damage. While the baseline raw FRF data (FS1) achieved a 99.84% accuracy, the distilled modal-based features performed comparably, with FS2 achieving 100% accuracy and FS3 reaching 99.52%. This confirms that the transition from high-dimensional raw FRF data to distilled modal features does not significantly compromise the model's diagnostic reliability. It suggests that the extracted features, particularly the FRF Peak Amplitude Ratio (PAR) in FS3, retain the essential physical characteristics required for the machine learning algorithm to differentiate between damaged states.

While accuracy remained consistently high across all sets, significant improvements were observed in computational overhead. The proposed feature set FS3 yielded the most compact model at 847 KB, representing a 35.0% reduction in storage requirements compared to the baseline FS1 (1,303 KB). This marginal improvement over FS2 (853 KB) indicates that the PAR feature allows for a slightly more efficient internal representation within the ML model.

In terms of training duration, FS3 recorded the lowest mean time at 33.38 seconds. This corresponds to an 18.64% reduction in training time relative to the baseline FS1 (41.03 seconds), whereas FS2 yielded an 8.19% reduction (37.67 seconds). While these absolute time savings are relatively small within this controlled laboratory setup, they do confirm a measurable improvement in basic computational efficiency for the proposed feature set.

**Table 3.** Feature set performance evaluation metrics.

| Feature Set | Features | Mean Model Size | Mean Training Duration | Prediction Accuracy |
|---|---|---|---|---|
| FS1 | FRF | 1,303 KB | 41.03 s | 99.84% |
| FS2 | WCC, FRF PA | 853 KB (-34.5%) | 37.67 s (-8.19%) | 100% |
| FS3 | WCC, FRF PAR | 847 KB (-35.0%) | 33.38 s (-18.64%) | 99.52% |

An analysis of the aggregated confusion matrices provides deeper insight into the class-wise classification performance. As depicted in Fig. 7, the minor accuracy drop in FS1 stems entirely from 4 instances where true LD-2 damage was misclassified as LD-1. Conversely, FS2 classified all samples across all folds correctly (Fig. 8). For the proposed feature set FS3, the confusion matrix (Fig. 9) reveals 12 total misclassifications strictly within the LD categories, specifically, 5 instances of true LD-1 predicted as LD-3, and 7 instances of true LD-3 predicted as LD-4. Notably, all misclassifications across the evaluated models were confined to the LD states. This indicates that while subtle structural changes at low damage severities are inherently the most challenging to distinguish, the proposed modal-based features still provide highly effective classification boundaries for UD, MD and HD.

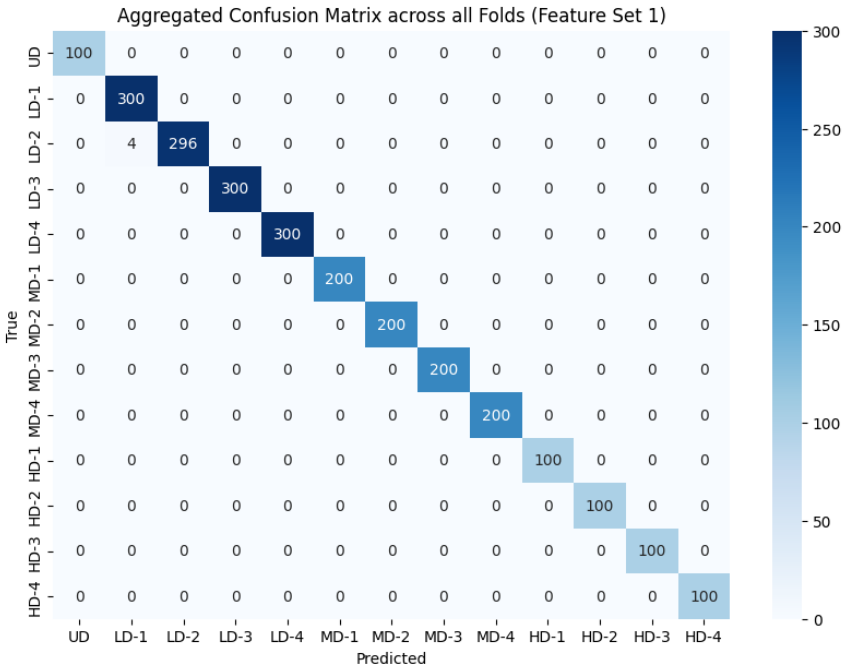


**Figure 7.** Aggregated confusion matrix across all fold (FS1).

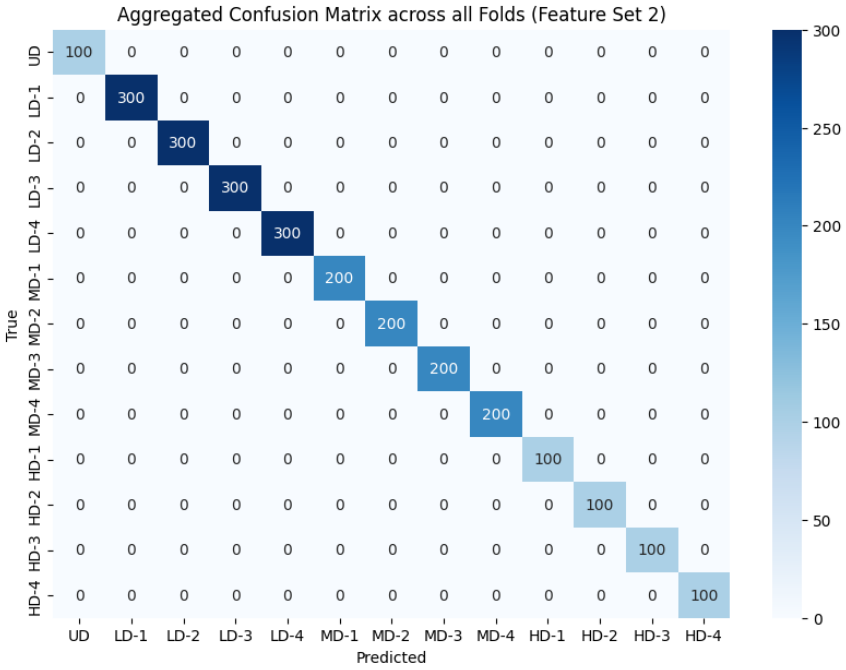


**Figure 8.** Aggregated confusion matrix across all fold (FS2).

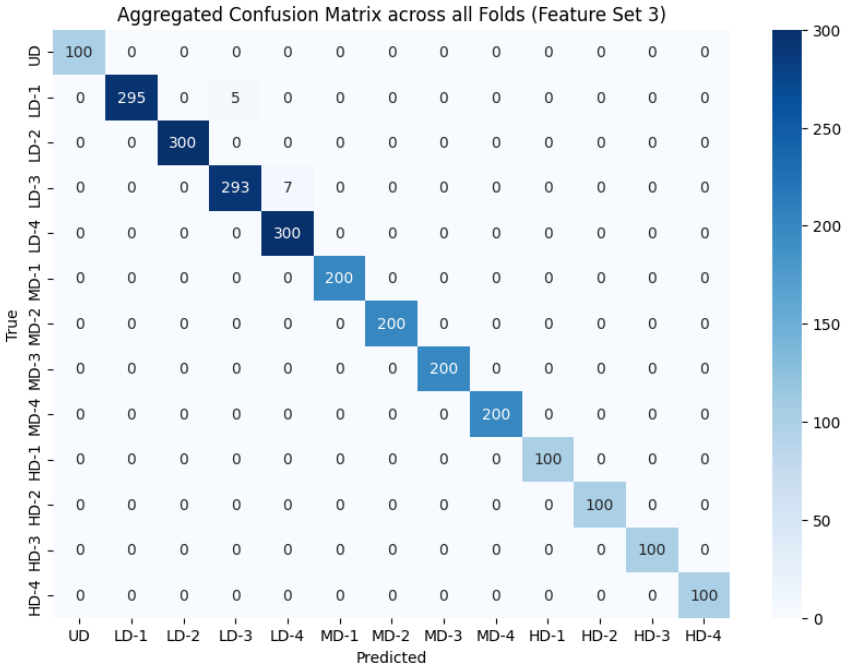


**Figure 9.** Aggregated confusion matrix across all fold (FS3).

## 4. Conclusion

This paper presented a comparative study on the efficacy of various feature sets for machine learning-based structural damage identification, with a specific focus on the novel FRF PAR. By transitioning from high-dimensional raw FRF to distilled vibration-based features, the research successfully addressed the common challenges of data bloat and computational latency in structural health monitoring.

The proposed feature set FS3 (WCC paired with FRF PAR) achieved a 99.52% prediction accuracy, proving that the reduction in data dimensionality does not sacrifice the model's ability to identify damage severity and location. Utilising FRF PAR resulted in the most efficient performance across all metrics, reducing the machine learning model size by 35.0% and training duration by 18.64% compared to utilising raw FRF. The reduction in storage and computational requirements benefits the integration of this approach into edge-computing devices. Future works will investigate the performance of this feature set by applying it in a hybrid digital twin framework to further validate its industrial viability.

## Acknowledgements

This work was supported by the Malaysian Ministry of Higher Education under the Fundamental Research Grant Scheme (No. FRGS/1/2022/TK10/UM/02/29). The authors also thank the Advanced Shock and Vibration Research (ASVR) Group, Universiti Malaya, for their contributions.

## References

Bitam, T., Yahiaoui, A., Boubiche, D. E., Martínez-Peláez, R., Toral-Cruz, H., & Velarde-Alvarado, P. (2025). Artificial Intelligence of Things for Next-Generation Predictive Maintenance. *Sensors*, 25(24), 67, Article 7636. https://doi.org/10.3390/s25247636

Cheah, B. Z., Ong, Z. C., Khoo, S. Y., Siow, P. Y., Ibrahim, Z., & Tan, C. G. (2025). Feasibility study of utilising modal-based features for finite element model-informed artificial neural network-based damage identification. In *Proceedings of the 11th International Operational Modal Analysis Conference (IOMAC 2025)* (pp. 392–399).

Chen, S. L., Ong, Z. C., Lam, W. H., Lim, K. S., & Lai, K. W. (2020). Unsupervised Damage Identification Scheme Using PCA-Reduced Frequency Response Function and Waveform Chain Code Analysis. *International Journal of Structural Stability and Dynamics*, 20(8), 26, Article 2050091. https://doi.org/10.1142/s0219455420500911

Li, J. C., Dackermann, U., Xu, Y. L., & Samali, B. (2011). Damage identification in civil engineering structures utilizing PCA-compressed residual frequency response functions and neural network ensembles. *Structural Control & Health Monitoring*, 18(2), 207-226. https://doi.org/10.1002/stc.369

Mardanshahi, A., Sreekumar, A., Yang, X., Barman, S. K., & Chronopoulos, D. (2025). Sensing Techniques for Structural Health Monitoring: A State-of-the-Art Review on Performance Criteria and New-Generation Technologies. *Sensors*, 25(5), 53, Article 1424. https://doi.org/10.3390/s25051424

Ruiz, D. V., Bragança, C. S. C. d., Poncetti, B. L., Bittencourt, T. N., & Futai, M. M. (2024). Vibration-based structural damage detection strategy using FRFs and machine learning classifiers. Structures, 59. https://doi.org/10.1016/j.istruc.2023.105753

Siow, P. Y., Ong, Z. C., Khoo, S. Y., Lim, K.-S., & Chew, B. T. (2023). Hybrid machine learning with mode shape assessment for damage identification of plates. *Smart Structures and Systems*, 31(5), 485-500. https://doi.org/10.12989/sss.2023.31.5.485